

LOW TEMPERATURE GROWTH OF ZINC OXIDE ON INSULATOR
UTILIZING GRAPHENE BUFFER LAYER FOR TRANSFERABLE
ELECTRONICS

‘AISAH MUHAMAD

UNIVERSITI TEKNOLOGI MALAYSIA

LOW TEMPERATURE GROWTH OF ZINC OXIDE ON INSULATOR
UTILIZING GRAPHENE BUFFER LAYER FOR TRANSFERABLE
ELECTRONICS

‘AISAH MUHAMAD

A thesis submitted in fulfilment of the
requirements for the award of the degree of
Doctor of Philosophy

School of Electrical Engineering
Malaysia-Japan International Institute of Technology
Universiti Teknologi Malaysia

NOVEMBER 2022

DEDICATION

To everyone

ACKNOWLEDGEMENT

I want to express gratitude to my supervisor, Prof Ts Ir Dr Abdul Manaf Hashim and my joint supervisor during my days in Japan, Prof Dr Kanji Yasui, for their priceless guidance, motivation, ideas, criticism, and wisdom. Through the study, I found that to be an excellent research; we we need to think out of the box, be indepensions, and believe in ourselves, not only for research but also in life. I am indebted to my supervisor, joint supervisor, and friends for their patience in sharing ideas and knowledge during the research.

Thankful to my fellow friends and seniors in Advanced Devices and Materials Engineering (i-Kohza). Besides sharing the ledge, they had assi me during the research and gave me a good moral to be a successful doctorate; they had become true friends, ys by my side either on 'sunny' or 'rainy' days.

Deep heart, I give heartiest thanks to my family, who always give moral support in becoming a good student and person in this life and hereafter.

Thank you and Alhamdulillah.

ABSTRACT

Intelligent system-on-chip (SoC), which is the heterogeneous integration of devices on insulator/silicon (Si) platform and other arbitrary substrates, is considered as the most promising next-generation technology. Since the insulator and those arbitrary substrates are generally amorphous, the direct growth of crystalline semiconductor materials is extremely difficult. Hence, a breakthrough of clever growth technology is demanded. Zinc oxide (ZnO) is one of the promising metal-oxide materials for many device applications like sensors, optoelectronic devices, etc. Buffer or template layer has been widely utilized to reduce the large lattice mismatch between the grown materials and insulators or arbitrary substrates. In this study, graphene, which is flexible, transparent and possesses a similar hexagonal atomic arrangement structure to ZnO, was chosen as a buffer or template layer. Since most of the arbitrary substrates possess low- melting temperatures, the growth of ZnO had to be performed at low temperatures. Three low- temperature techniques were used; combination of thermal evaporation and oxidation, hydrothermal deposition and hot-water-beam chemical vapour deposition (CVD). For thermal evaporation, first, ZnO film with a thickness of ~350 nm was deposited, followed by oxidation treatment at 450°C in oxygen ambient. The oxidation times varied between 30 to 120 minutes. Oxidation of physically deposited ZnO was to minimize the oxygen vacancies or to increase the crystallinity of ZnO with the appearance of diffraction peaks corresponded to (0002), (10-10) and (10-11), and these peaks increased with the oxidation time up to 60 min. However, the peak intensity showed a decrease with broad FWHM of (0002) after 60 min of oxidation which was speculated to be caused by the intermixing of ZnO and graphene. For the hydrothermal process, which was carried at 90°C for 3 hours, a graphene/glass and a ZnO/ glass were used as the substrates. No growth of ZnO was obtained on graphene/glass. It was speculated that graphene with low defects might not promote the nucleation of ZnO. However, the growth of ZnO nanorods on ZnO-seeded was obtained with a considerable small FWHM of 0.2892° for the (0002) peak. However, the intensity ratios of the ultraviolet emission (I_{uv}) and visible emission (I_{vis}) for both ZnO grown by thermal evaporation combined with oxidation, and hydrothermal process were around 1.05. This suggested that defects or oxygen vacancies were still high. Finally, ZnO was grown on graphene/SiO₂/Si by hot water beam CVD with a growth time ranging from 20-60 min at a fixed substrate temperature of 500°C. As expected, a ZnO layer with high crystallinity (small FWHM of 0.0743°- 0.1955° for the (0002)) was obtained. Since the location of the 2θ of ZnO (0002) was close to the bulk value, this seemed to suggest less residual tensile stress compared to the other two methods. Extremely low defect of CVD-grown ZnO layer was also confirmed from I_{uv}/I_{vis} measurement, suggesting the potential for the device fabrication. The use of graphene as the buffer or template layer provides the potential for transferable electronics since the adhesion of graphene and substrate is extremely weak.

ABSTRAK

Sistem-pada-cip (SoC) pintar, yang merupakan peranti penyepaduan heterogen pada pelantar penebat/silikon (Si) dan substrat sebarang yang lain, telah dianggap sebagai teknologi generasi-masa-depan yang memberangsangkan. Pertumbuhan langsung bahan semikonduktor kristal amat sukar disebabkan oleh penebat dan substrat sebarang yang secara umumnya amorfus. Jadi, suatu kejayaan teknologi pertumbuhan yang bijak adalah dituntut. Zink oksida (ZnO) merupakan salah satu bahan logam-oksida yang menggalakkan untuk diaplikasikan pada banyak peranti seperti penerima, peranti optoelektronik, dan lain – lain. Lapisan penampan atau templat telah digunakan secara meluas bagi mengurangkan ketakpadanan kekisi yang ketara di antara bahan yang ditanam dan penebat atau substrat sebarang. Dalam kajian ini, grafin, yang fleksibel, telus dan mempunyai struktur susunan atom heksagon yang sama dengan ZnO, telah dipilih sebagai lapisan penampan atau templat. Disebabkan kebanyakan substrat sebarang mempunyai suhu lebur yang rendah, pertumbuhan ZnO perlu dilakukan pada suhu rendah. Tiga teknik suhu rendah telah digunakan; gabungan penyejatan terma dan pengoksidaan, pemendapan hidroterma dan alur air panas pemendapan wap kimia (CVD). Untuk penyejatan terma, pertama, filem ZnO dengan ketebalan ~ 350 nm diendapkan, diikuti dengan rawatan pengoksidaan pada 450°C dalam ambien oksigen. Masa pengoksidaan diubah, antara 30 hingga 120 minit. Pengoksidaan ke atas endapan fizikal ZnO adalah bagi meminimumkan kekosongan oksigen atau untuk meningkatkan kehabluran ZnO dengan mempamerkan puncak pembelauan yang sepadan dengan (0002), (10-10) dan (10-11), dan puncak-puncak ini telah meningkat dengan masa pengoksidaan sehingga 60 minit. Namun, keamatan puncak menunjukkan penurunan dengan FWHM (0002) yang lebar selepas 60 minit pengoksidaan yang dijangka disebabkan oleh percampuran diantara ZnO dan grafin. Bagi proses hidroterma, yang telah dilakukan pada suhu 90°C selama 3 jam, grafin/kaca dan ZnO/kaca telah digunakan sebagai substrat. Tiada pertumbuhan ZnO diperoleh pada grafin/kaca. Ini berkemungkinan disebabkan oleh kecacatan yang rendah pada grafin yang mungkin tidak merangsang nukleasi ZnO. Namun, FWHM yang kecil terhasil daripada pertumbuhan nanorod ZnO pada ZnO-biji iaitu 0.2892° bagi puncak (0002). Walau bagaimanapun, nisbah keamatan pancaran ultraviolet (I_{uv}) dan pancaran nampak (I_{vis}) bagi kedua-dua ZnO yang ditanam melalui gabungan penyejatan terma dan pengoksidaan, dan proses hidroterma adalah sekitar 1.05. Ini menunjukkan bahawa kecacatan atau kekosongan oksigen masih tinggi. Akhirnya, ZnO ditanam pada grafin/SiO₂/Si oleh alur air panas CVD dengan masa pertumbuhan diantara 20-60 min pada suhu substrat yang tetap, 500°C . Seperti yang dijangkakan, lapisan ZnO dengan kehabluran tinggi (FWHM kecil 0.0743° - 0.1955° bagi (0002)) telah diperoleh. Memandangkan lokasi 2θ ZnO (0002) berhampiran dengan nilai pukal, ini menunjukkan tegasan tegangan sisa yang kurang berbanding dengan dua kaedah lain. Kecacatan yang sangat rendah pada lapisan ZnO yang ditanam CVD juga telah disahkan daripada pengukuran $I_{\text{uv}}/I_{\text{vis}}$, menunjukkan potensi bagi fabrikasi suatu peranti. Penggunaan grafin sebagai lapisan penampan atau templat adalah berpotensi untuk elektronik berpindah kerana lekatan grafin dan substrat adalah sangat lemah.

TABLE OF CONTENTS

	TITLE	PAGE
	DECLARATION	i
	DEDICATION	ii
	ACKNOWLEDGEMENT	iii
	ABSTRACT	iv
	ABSTRAK	v
	TABLE OF CONTENTS	vi
	LIST OF TABLES	ix
	LIST OF FIGURES	x
	LIST OF ABBREVIATIONS	xiii
	LIST OF SYMBOLS	xvi
CHAPTER 1	INTRODUCTION	1
1.1	Research Background	1
1.2	Research Motivation	3
1.3	Problem Statement	8
1.5	Research Objective and Scopes	10
1.6	Overview of Thesis Organization	12
CHAPTER 2	LITERATURE REVIEW	15
2.1	Introduction	15
2.2	Materials Properties of ZnO	16
2.2.1	Structural Properties of ZnO	16
2.2.2	Basic Properties of ZnO	18
2.2.3	Electrical Properties of ZnO	19
2.2.4	Optical Properties of ZnO	19
2.3	Material Properties of Graphene	21
2.3.1	Structural Properties of Graphene	22

2.4	Utilization of Buffer Layer for Growth of ZnO in Insulator and Its Potential Applications	23
2.5	Growth Methods of ZnO Nanostructures	25
2.5.1	Thermal Evaporation Growth of ZnO	29
2.5.2	Hydrothermal Growth of ZnO Nanostructures	30
2.5.3	CVD Growth of ZnO Structures using High-Temperature Platinum Catalyzed Water Beam (Hot Water Beam CVD)	32
2.6	Summary	33
CHAPTER 3	RESEARCH METHODOLOGY	35
3.1	Introduction	35
3.2	Research Activities	35
3.3	Properties of the substrate	38
3.3.1	Glass slides	38
3.3.2	Graphene on insulator	38
3.4	Deposition of ZnO film on insulator using thermal evaporator PVD	43
3.4.1	Deposition of ZnO film on graphene/insulator	43
3.4.2	Oxidation of ZnO film and its parameter	45
3.5	Growth of ZnO structures on insulator using hydrothermal method.	47
3.6	Growth of ZnO /graphene structures on insulator using hot water beam CVD	50
3.6.1	Structure of hot water beam CVD system and its working principle for the growth of ZnO thin film on graphene on insulator	50
3.6.2	Growth parameter	54
3.7	Characterization and Analysis of Grown ZnO	55
3.7.1	Morphology and Composition of ZnO Thin Film	55
3.7.2	Crystallinity of ZnO	58
3.7.3	Optical Properties of ZnO	60
3.8	Summary	61
CHAPTER 4	SYNTHESIS OF ZNO THIN FILMS ON INSULATOR UTILIZING GRAPHENE BUFFER LAYER USING A	

	COMBINATION OF THERMAL EVAPORATION AND OXIDATION PROCESS	62
4.1	Introduction	62
4.2	Morphology of ZnO As-deposited and Oxidized ZnO Thin Films	62
4.3	Crystallography of ZnO Thin Films on Insulator	67
4.4	Optical Properties of ZnO on Graphene on Insulator	73
4.5	Summary	78
CHAPTER 5	GROWTH OF ZNO ON BUFFER LAYER ON INSULATOR USING HYDROTHERMAL TECHNIQUE	80
5.1	Introduction	80
5.2	Morphological Properties of ZnO Nanorods on Insulator	80
5.3	Optical Properties of ZnO on Insulator	84
5.4	Crystallography Properties of ZnO on Insulator	86
5.5	Summary	87
CHAPTER 6	GROWTH OF ZNO ON GRAPHENE ON INSULATOR USING HIGH-TEMPERATURE PLATINUM-CATALYZED WATER BEAM	89
6.1	Introduction	89
6.2	Morphological Properties of ZnO on Insulator with Graphene Buffer Layer	89
6.3	Crystallography Properties of ZnO on Graphene Buffer Layer	92
6.4	Optical Properties of ZnO on Graphene Buffer Layer	96
6.5	Summary	101
CHAPTER 7	CONCLUSION AND FUTURE WORK	105
7.1	Contributions of Present Work	105
7.2	The direction of Future Work	107
7.3	Summary	108
	REFERENCES	109
	LIST OF PUBLICATIONS	130

LIST OF TABLES

TABLE NO.	TITLE	PAGE
Table 2.1	Physical parameters of ZnO at room temperature	18
Table 3.1	Growth Parameter	55
Table 5.1	Density, average length and diameter, aspect ratio and energy bandgap from PL spectra and transmittance of the grown ZnO nanorods on the ZnO seed layer.	86
Table 6.1	Buffer type, method, structure, thickness, growth rate, FWHM at ZnO (002), grain size, energy bandgap from PL and transmittance, and intensity ratio of ZnO grown on buffer layer on insulator	103

LIST OF FIGURES

FIGURE NO.	TITLE	PAGE
Figure 1.1	Evolution of Si in ‘More than Moore’ [15]	2
Figure 1.2	Different types of leakage current present in transistor [31]	3
Figure 2.1	Crystal structure of hexagonal wurtzite ZnO [76]	17
Figure 2.2	Photoluminescence spectra of ZnO	20
Figure 2.3	Forms of sp ₂ -bonded carbon of (a) graphite, (b) graphene, (c) carbon nanotube and (d) fullerene [87].	21
Figure 2.4	Honeycomb lattice of graphene	23
Figure 2.5	Schematic for the synthesis of ZnO nanostructures	26
Figure 2.6	Mechanism of deposition of metal oxide by sputtering PVD [108]	27
Figure 2.7	(a) Schematic of spray system (b) Schematic of the nucleation and growth process in the system [109]	28
Figure 2.8	Sol-gel technique for chemical production of ZnO nanoparticles [107]	29
Figure 2.9	A schematic of the growth mechanism of CVD-grown ZnO used as the nucleation site for the subsequent hydrothermally grown ZnO film [44].	33
Figure 3.1	Research flowchart	37
Figure 3.2	FESEM images of (a) SLG and (b) MLG on insulator	39
Figure 3.3	(a) Nomarski image and Raman mapping of SLG and (b) Raman spectra for as-received SLG on insulator at RT	41
Figure 3.4	(a) Nomarski image and Raman mapping of MLG and (b) Raman spectra for as-received MLG on insulator at RT	43
Figure 3.5	(a) Schematic diagram of thermal evaporator PVD and (b) Deposited ZnO on the substrate	44
Figure 3.6	The schematic of the ZnO oxidation process using the dual-zone furnace	45
Figure 3.7	Time chart for ZnO structures oxidation process	46
Figure 3.8	Schematic of hydrothermal deposition setup	48

Figure 3.9	Temperature-time profile of hydrothermally grown ZnO structures	49
Figure 3.10	Schematic diagram of hot water beam CVD setup	51
Figure 3.12	Substrate clipped on ceramic heater set up	53
Figure 3.13	Temperature-voltage calibration of hot water beam CVD	53
Figure 3.14	Schematic diagram of AFM	56
Figure 3.15	Schematic diagram of Fesem-EDX	58
Figure 3.16	Bragg's reflection of X-rays from two planes of atom in a crystal solid	59
Figure 3.17	Schematic of the photoluminescence excitation [142]	60
Figure 4.1	The FESEM image of (a) as-deposited ZnO and (b) as-deposited ZnO on graphene on insulator, (Insert) The sample's surface of as-deposited ZnO film.	63
Figure 4.2	The FESEM images (top and cross-section) of ZnO on the insulator with (a) 30, (b) 60 and (c) 120 minutes of oxidation time, and (Insert) the sample's surface of ZnO/insulator after oxidation.	65
Figure 4.3	The FESEM images (top and cross-section) of ZnO on graphene on the insulator with (a) 30, (b) 60 and (c) 120 min of oxidation time, (Insert) The sample's surface of ZnO/graphene/insulator after oxidation.	66
Figure 4.4	XRD patterns of the deposited ZnO thin films on (a) insulator and (b) graphene/insulator with different oxidation times at 450°C.	69
Figure 4.5	The graph of FWHM of XRD (0002) and grain size versus thickness of deposited ZnO on (a) glass and (b) graphene/glass	71
Figure 4.6	PL spectra of deposited ZnO on (a) insulator and (b) graphene/insulator with various oxidation times	74
Figure 4.7	Transmittance spectra of deposited ZnO on (a) insulator and (b) graphene/insulator	76
Figure 4.7	Transmittance spectra of deposited ZnO on (a) insulator and (b) graphene/insulator (continued)	77
Figure 5.1	FESEM image (top and cross-sectional view) of ZnO been grown on (a) SLG, (b) MLG and (c) ZnO seed on insulator	83
Figure 5.2	Photoluminescence spectra of ZnO on insulator with the varying buffer layer	84

Figure 5.3	XRD patterns of grown ZnO on ZnO seed layer on the insulator	87
Figure 6.1	The FESEM images (top and cross-sectional view), AFM images and EDX spectra of the ZnO films grown on (a) SLG and (b) MLG with 60 minutes growth time.	91
Figure 6.2	XRD patterns of the grown ZnO thin films on (a) SLG and (b) MLG at temperatures of 500°C	93
Figure 6.3	(a) FWHM versus thickness, and (b) grain size versus thickness of ZnO films grown on both SLG and MLG	95
Figure 6.4	PL spectra of ZnO films grown on (a) SLG and (b) MLG measured at room temperature (RT)	97
Figure 6.5	Transmittance spectra of ZnO films on SLG	99
Figure 6.6	Relationship between growth rate and growth time (Insert) R_a vs growth rate	100

LIST OF ABBREVIATIONS

0D	-	Zero dimensional
1D	-	One dimensional
2D	-	Two dimensional
3D	-	Three dimensional
AFM	-	Atomic force microscopy
AI	-	Artificial intelligent
Ar	-	Argon
a-Si:H	-	Hydrogenated amorphous silicon
CdO	-	Cadmium oxide
CH ₂ O	-	Formaldehyde
CMOS	-	complementary metal-oxide-semiconductor
Cu	-	Copper
CuO	-	Copper oxide
CVD	-	Chemical vapor deposition
DI	-	Deionized
DLE	-	Deep level emission
DMZn	-	dimethyl zinc
EDX	-	Energy dispersive x-ray
FESEM	-	Field emission scanning electron
FET	-	Field effect transistor
FWHM	-	full width half maximum
GaAs	-	Gallium arsenide
GaN	-	Gallium nitride
Ge	-	Germanium
H ₂	-	Hydrogen
H ₂ O	-	Water
hBN	-	Hexagonal boron nitride
HMTA	-	Hexamethylenetetramine
IoT	-	Internet of thing
IR	-	Infrared

ITO	-	Indium tin oxide
LP-MOCVD	-	Low-pressure metal-organic chemical vapor deposition
MBE	-	Molecular beam epitaxy
MgO	-	Magnesium oxide
MLG	-	Multilayer graphene
MOCVD	-	Metal-oxide chemical vapor deposition
MoS ₂	-	Molybdenum disulphide
N ₂	-	Nitrogen
N ₂ O	-	Nitrous oxide
NBE	-	Near band edge
NH ₃	-	Ammonia
NH ⁴⁺	-	Ammonium
O	-	Oxygen (atom)
O ₂	-	Oxygen (molecule)
O ²⁻	-	Oxygen ion
OH ⁻	-	Hydroxyl
PL	-	Photoluminescence
Pt	-	Platinum
PVD	-	Physical vapor deposition
rGO	-	Reduced graphene oxide
RF	-	Radiofrequency
RMS	-	Root mean square
RT	-	Room temperature
Si	-	Silicon
Si-ULSi	-	Silicon-ultra-large-scale
SiC	-	Silicon carbide
Si ₃ N ₄	-	Silicon nitrate
SiO ₂	-	Silicon dioxide
SLG	-	Single-layer graphene
TEM	-	Transmission electron microscope
ULSi	-	Ultra-large-scale integrated circuit
UV	-	Ultraviolet
UV-Vis	-	Ultraviolet-visible

vdW	-	Van der Waals
XRD	-	X-ray diffraction
Zn	-	Zinc
Zn ²⁺	-	Zinc ion
Zn(CH ₃) ₂	-	Dialkyl Zinc
Zn(NO ₃) ₂ ·6H ₂ O	-	Zinc nitrate hydroxide
ZnO	-	Zinc oxide
ZrO ₂	-	Zirconia
ZnS	-	Zinc sulphide

LIST OF SYMBOLS

λ	-	Lambda
μm	-	Micrometre
$^{\circ}$	-	Degree
$^{\circ}\text{C}$	-	Degree Celsius
\AA	-	Angstroms
a. u.	-	Arbitrary unit
cm	-	Centimetre
cm^2/Vs	-	Centimetres squared per volt-second
cm^{-1}	-	Per centimetre
cm^{-3}	-	Per centimetre cube
d	-	Interplanar spacing
eV	-	Electron volt
Hz	-	Hertz
$I_{\text{uv}}/I_{\text{vis}}$	-	Intensity of UV emission to intensity of green emission
meV	-	Milli-electron volt
min	-	Minute(s)
ml	-	Millilitre
mM	-	Millimolar
ms	-	Millisecond
n	-	Integer
nm	-	Nanometer
Pa	-	Pascal
sccm	-	Standard cubic centimetre per minute
W/mK	-	Watt per metre Kelvin
O_i	-	Oxygen interstitial
V_o	-	Oxygen vacancy
V_{Zn}	-	Zinc vacancy
Zn_i	-	Zinc interstitial
%	-	Percentage
θ	-	Angle

CHAPTER 1

INTRODUCTION

1.1 Research Background

People nowadays live in a modern era where the use of nano-sized silicon-based transistors has brought the realization of the Internet of Things (IoT) and artificial intelligence (AI) technology. The revolution of Silicon (Si) based transistor that kept growing over the years, together with the size reduction of the transistor, allowed the miniaturization of the transistor, which enables numbers of transistors to be crammed onto a single Si platform, thereby boosting computer capabilities. This obeyed Moore's law, where the performance of silicon-ultra-large-scale integrated circuits (Si-ULSIs) has been improved over the last 30 years by doubling the number of transistors every two years on a single platform [1]. Today, a single processor can hold more than a trillion transistors [2]. However, the never-ending miniaturization of transistors makes winning more difficult due to limitations such as the short channel effect and gate leakage current.

The concept of advanced heterogeneous integration on a single platform has attracted much attention toward realizing a 'More than Moore' technology [3]. In realizing such technology, the growth of various high-quality semiconductors such as germanium (Ge) [4], gallium arsenide (GaAs) [5], gallium nitride (GaN) [6], silicon carbide (SiC) [7], zinc oxide (ZnO) [8] on the platform is a must. The co-integration of materials enables the present ULSIs to be facilitated not only with ultra-high-speed complementary metal-oxide-semiconductor (CMOS) transistors and novel transistors [9] but also with various kinds of functional devices, such as optical devices [10], photodetectors [11], solar batteries [12], and sensors [13, 14]. Such intelligent system-on-chip (i-SoC) on Si is considered a promising and practical direction. To fabricate multi-functional devices on a single Si substrate, it is necessary to electronically isolate the semiconductor materials using insulators such as silicon dioxide (SiO₂), silicon

nitride (Si_3N_4) or arbitrary substrates. Figure 1.1 illustrates the evolution of Si in the ‘More than Moore’ [15]. However, the hybridization of high performance of semiconductors and insulators is impossible due to the amorphous structures of the insulators. Therefore, it needs some significant development in growth technology.

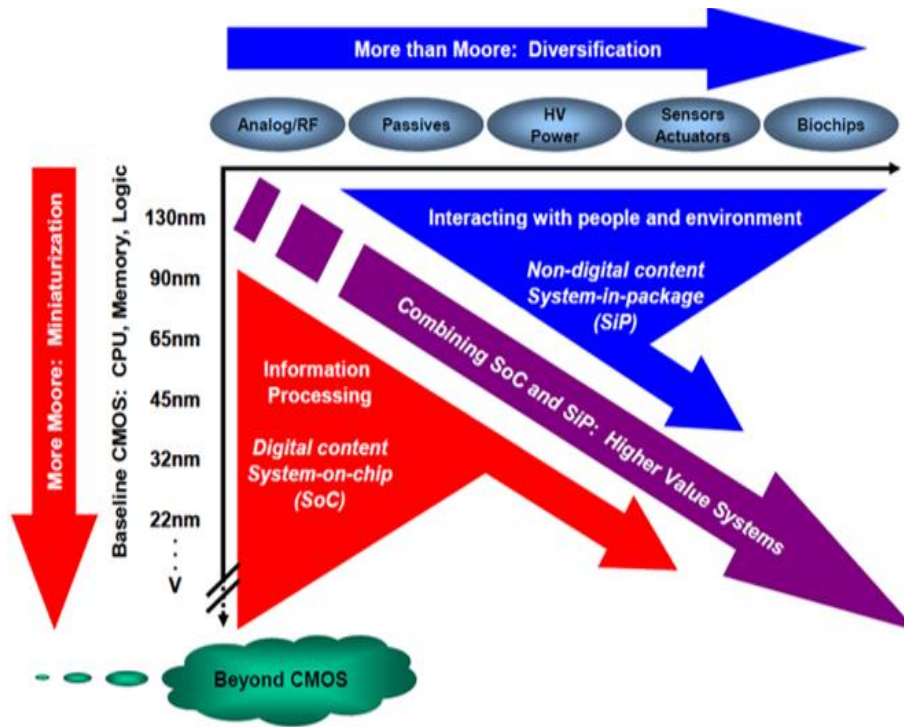


Figure 1.1 Evolution of Si in ‘More than Moore’ [15]

In the meantime, the use of insulators or arbitrary substrates such as polymers, rubber, and glass to fabricate the devices has become phenomenal today. Some of the devices are widely used in optoelectronics [16-18], sensors [19-21], and photovoltaic [22, 23] industries. Several advantages include simple, environmentally friendly, yet cheap materials suitable for the fabrication of commercial devices. Besides, other physically unique and eye-catching features like flexibility, transparency, and colourful are added values for device production on these arbitrary platforms. However, it still needs technology to breakthrough in fabricating semiconductor devices on these platforms due to the substrate's non-crystalline or amorphous structure, which makes the fabrication of high-quality semiconductor devices challenging.

Graphene is remarkably known for its flexibility and has superior characteristics. Besides, it has a similar hexagonal orientation to the ZnO, making a combination of ZnO and graphene feasible. Hence, in this study, we will utilize graphene as the buffer layer for ZnO on the insulator, and we speculate that the grown ZnO structures on the insulator by using graphene as the template or buffer layer will be high-quality.

1.2 Research Motivation

Since decades ago, semiconductor materials such as ZnO, SiC, GaN and GaAs have been widely used in device fabrication, such as in sensors [24-26], transistors [27], optoelectronics [28, 29] and photovoltaic [30]. Generally, the materials' morphology, compositions, and physical and chemical properties can be controlled during the growth process, which can be exploited for specific device fabrication. However, in fabricating a semiconductor device system on a Si substrate, it is crucial to electronically isolate the grown material and Si platform with any isolator, such as SiO₂, Si₃N₄, or any arbitrary substrate, to avoid any current leakage or short circuit, especially in the production of CMOS or field-effect transistor (FET) as in Figure 1.2 [31]. On the other hand, a recent commercial-value semiconductor device was fabricated on a cheap and flexible platform like polymers and glass.

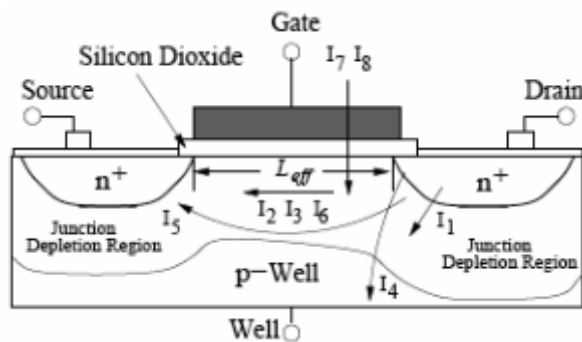


Figure 1.2 Different types of leakage current present in transistor [31]

The concept of flexible electronics device fabrication was introduced in the 1960s [32]. It begins with thinned-Si platforms, which have been used in solar cell fabrication for extra-terrestrial satellites. Over the years, researchers have added some

exciting features in fabricating flexible yet lightweight devices, such as increasing their robustness and stretchability. This device must be robust in order to avoid any deformation or malfunction during the integration process. These unique characteristics will eventually increase semiconductor electronic devices' quality, sensitivity, and performance. Aside from thinned-Si, some other inexpensive arbitrary substrates were used as the platform, such as polymers [33, 34], hydrogenated amorphous Si (a-Si:H) [35], and glass [36], which brought out visually appealing features like transparent, bendable and flexible [37]. The semiconductor-based flexible electronics have grasped attention throughout these years due to their wide-ranging applications, such as flexible displays [33] and skin electronics [38].

Recently, some novel technology for fabricating semiconductor-based flexible electronics device systems with an ability to be transferred from one platform to another has arisen. This process usually uses an atomically thin layer of two-dimensional (2D) materials or novel van der Waals (vdW) heterostructures as the transferred tool or template layer [39]. These thin layers of 2D materials such as graphene [40], molybdenum disulfide (MoS_2) [41], or hexagonal boron nitride (hBN) [39, 41], which act as the template will allow the metal-oxide to be directly grown on that template, where it will be part of the device. This innovative technology trend enhanced i-SoC on the semiconductor or arbitrary platform's performance to the full extent with the versatility of device fabrication technique.

In realizing a good performance of flexible and transferable semiconductor-based electronic devices on the insulator-character arbitrary substrate, it is essential to do a fundamental study, beginning with the growth process of semiconductor materials. A breakthrough in growth technology is strongly required to fabricate a high-quality semiconductor-on-insulator with excellent crystallinity and other properties. Since an insulator has amorphous or polycrystalline lattice structures, growing the high crystallinity of semiconductor structures on an insulator is almost impossible. It is because of the large lattice mismatch between a crystalline semiconductor and an amorphous insulator [42]. This significant lattice difference will make the grown semiconductor material in the polycrystalline structure; thus, making a high-quality semiconductor structure is challenging. In reducing the lattice

mismatch, a buffer or template layer is exploited during fabrication [43]. Similar to the fabrication of transferable devices, this template layer for the growth of high-quality semiconductor structures on the insulator was placed between semiconductor materials and the insulator. In addition, some growth methods also need a buffer layer of semiconductor materials for the nucleation site of the subsequent material growth, such as in the hydrothermal growth technique [44].

Several intensive researchers have focused on fabricating one and two-dimensional ZnO semiconducting nanostructures throughout the years because of their uniqueness in morphology, compositional and other main properties such as chemical, physical, optical and electrical. This white and non-toxic ZnO is a promising candidate for the fabrication of several devices due to its unique electronic and optical properties, such as a wide bandgap at 3.37 eV and enormous exciton binding energy of 60 meV at room temperature (RT) [45, 46]. These properties allow the ZnO-based devices to be used at RT without any hindering from thermal instability. In addition, the high transparency of ZnO makes it the best choice for making transparent-like devices such as photovoltaics. Thus, ZnO is the best material for the device's system in various astonishing applications such as photovoltaics, optoelectronics, and sensor sensing elements [47].

As mentioned, a template layer is needed during the growth process of ZnO on an insulator, the type of material used for the template layer is also critical, starting with lattice orientation. The lattice orientation of both the template layer and semiconductor is preferably similar. Here, the lattice of both template and insulator will bond together using vdW forces by mechanically-assembled stacks or physical epitaxy or chemical vapor deposition (CVD) [39]. One of the simplest ways to grow ZnO structures on the template is by using the same material, ZnO-seed, as the buffer layer. The exact similar lattice structure will eventually make a least lattice mismatch. This ZnO layer, known as the ZnO seed layer, is commonly used as the nucleation site to enable the subsequent growth of ZnO nanostructures on the insulators [44]. Still, using the ZnO thin layer as a template layer is challenging for fabricating flexible and transferable devices [48]. Those very fragile materials give some minus points for the fabrication of a transferable device as it may be deformed during transferring process

of the device. Here, atomically thinned 2D material with a similar lattice orientation to the ZnO, such as graphene, is the best candidate to act as the buffer layer.

Graphene is a 2D hexagonal network of carbon atoms formed by making strong triangular σ -bonds of the sp^2 -hybridized orbitals. This bonding structure is similar to the (111) plane of zinc-blende and the c-plane of a hexagonal crystalline structure [49]. Thus, making the growth of semiconductor nanostructures and thin films on graphene feasible. In addition, graphene has excellent potential for novel electronic devices because of its extraordinary optical, electrical, thermal, and mechanical properties, including carrier mobility exceeding 10^4 cm^2/Vs and thermal conductivity of 10^3 W/mK [49].

This zero bandgap and high mobility of graphene can also act as the metal contact or junction, allowing electrons or ions to move freely from one place to another. Therefore, with such excellent characteristics of graphene layers, growing semiconductor nanostructures on graphene layers would enable their novel physical properties to be exploited in diverse, sophisticated device applications. Since graphene is an excellent heat conductor thus, a significant issue of thermal management in heterogeneous integration can also be solved. In addition, the weakly bonded layers of graphene allow transferring the grown semiconductor nanostructures or films onto other arbitrary substrates such as glass, metal, and plastics [37]. Hence, we speculated that using this atom-thick material with high flexibility, transparency, and mobility as the buffer layer would likely increase the quality of grown ZnO.

Diverse group morphologies of ZnO structures such as nanorods [50], nanowires [51], nano-porous [52] and thin films [44] were synthesized using a variety of vapor and liquid phase fabrication techniques. In addition, the vapor phase deposition techniques can be separated into two; physical vapor deposition (PVD) and CVD. These deposition methods include metal-oxide chemical vapor deposition (MOCVD), molecular beam epitaxy (MBE), and thermal evaporation, while the liquid phase techniques include hydrothermal, sol-gel deposition and electrodeposition [53]. Each method has its benefits in growing the ZnO structures on a substrate.

PVD methods can be either sputtering, thermal evaporators or others. In some cases, the PVD technique is preferable over CVD due to its advantages, such as fast growth and simplicity. Besides, this technique only uses a single solid target. Again, some methods like electron beam and thermal evaporation have no direct temperature applied on the substrates, making it possible to be carried on the substrates with low-melting temperatures, such as plastic or rubber. In addition, the process is considered less toxic, so there will be no toxic waste, such as toxic gas or liquid, throughout the experiment. Therefore, this study will use thermal evaporation as the only PVD-based method for depositing the ZnO on the insulator at low temperatures.

On the other hand, implementing the liquid phase of the chemical approach as the growth technique is still impossible for industrial-scale production. However, this technique fits for studying the grown semiconductor on an insulator utilizing a buffer layer. Simple, low operating temperatures, yet a wide range of chemicals can be used as the aqueous solutions and electrolytes throughout the process. Thus, it allows the study on the effect of the buffer layer on the grown structures.

Meanwhile, MOCVD has a higher commercial value than other methods because it can grow high-quality nanostructures compared to liquid phase deposition techniques and has cheaper production than the MBE technique. The ability of these methods to coat the unreachable area and evenly coated irregular surfaces is preferable in the coating industry. Besides, it can grow at a large scale with a wide range of elements and compounds with a high-purity end product, making the technique suitable for the industrial scale. However, MOCVD tends to have high energy consumption and higher toxicity due to precursors in metal oxides and waste products. These pros and cons of techniques have initiated researchers to upgrade and invent an innovative approach that can increase production quality and commercial value at a low cost.

One of the innovative technologies is a high-temperature water CVD known as hot water beam CVD. Yasui et al. invented this technique for overcoming the high energy consumption problem using conventional CVD. The hot water CVD used high energy of water molecules originated from the exothermic reaction of H_2 and O_2 . Then,

the hot H₂O will react with the Zn source to produce ZnO molecules, which then been directly grown on the substrate. Although the research study of grown material in film and nanostructures using this technique is still at the surface, continuous results show that the technique can overcome past problems in using conventional CVD, such as high power consumption and toxic gas [54]. Besides, this technique uses a low working temperature and pressure, suitable for pressure and temperature-sensitive materials such as a polymer.

In this study, the deposition of ZnO structures on an insulator with graphene as a buffer layer is carried out by a combination of thermal evaporation and oxidation. The deposition process was carried out using the thermal evaporation technique under vacuum conditions, with ZnO powder as the main target. Next, the deposited ZnO layer was annealed under an oxygen (O₂) ambient. Only one parameter was used to optimize the oxidation condition, which is the oxidation time, that acted on ZnO with and without buffer layers. Besides, the physically deposited ZnO will be utilized as the buffer layer to study the growth of ZnO structures using the liquid phase of the chemical approach; the hydrothermal method. The outcomes are compared with the hydrothermally grown ZnO structures on an insulator utilizing single-layer graphene (SLG) and multi-layer graphene (MLG). These buffer layer differences are expected to play a role in the growth of ZnO structures. The recent vapor phase CVD technique, hot water beam CVD, grows ZnO structures on SLG and MLG insulators. Here, the number of graphene layers and the growth time were differentiated. Finally, grown ZnO structures' morphological, crystallinity and optical properties are systematically characterized.

1.3 Problem Statement

The use of high crystalline semiconductor material in fabricating optoelectronics and photovoltaic applications has been started for years. Over the last decades, heterogeneous integration technology has been promising in realising the next-generation technology, the so-called i-SOC. However, in realizing such technology, it is crucial to isolate the active semiconductor and the Si platform to avoid

any current leakage or short circuit. It has brought the introduction of the insulator to many multifunctional devices such as power devices, electronic displays and so forth. In the meantime, arbitrary substrates, such as polymer, glass and paper, were introduced to replace the conventional Si in fabricating electronic devices, where these substrates had some unique features such as flexibility and transparency. And recently, the emergence of transferable electronics that can be transferred between the arbitrary substrate, such as LED, utilised template or buffer layers during device fabrication.

ZnO, an II-VI element, is given high interest to be studied for its wide bandgap and large exciton energy. These behaviours allow the ZnO-based device to work well at room temperature and have a higher breakdown voltage. Moreover, ZnO has high transparency, can be implemented for the element in a transparent device and is environmentally friendly. However, a significant lattice mismatch has made a direct growth of crystalline ZnO on the insulator almost impossible. Here, a buffer layer such as graphene and hBN with a similar hexagonal lattice structure with the ZnO was introduced to reduce the lattice difference. However, graphene consists of a single element, robust, flexible and transparent, and has zero bandgap that can be exploited as the active element, is the best choice as the buffer or template layer. Thus, in this case, the use of graphene is favourable due to the similar hexagonal lattice structure with the ZnO and the graphene's superior characteristics, such as good conductivity, which are expected to enhance the performance of the semiconductor ZnO on the insulator. However, some arbitrary substrates, such as polymer or paper, have low thermal resistance, which becomes a critical issue in the growth process. Therefore, the low-temperature technique is needed.

Thus, we need a breakthrough in the growth technique, where the growth processes are focused on low-temperature growth at less than 600°C. Several techniques for the growth process are covered in physical and chemical approaches. PVD and CVD are common techniques used on a commercial scale, and one of the simple yet well-known liquid phases using a chemical approach is hydrothermal. In this study, the thermal evaporation PVD with a combination of oxidation at low temperatures will be used as one of the growth techniques. One of the CVD techniques, hot water beam, is one of the latest techniques which focuses on low-temperature

growth with simple H₂ and O₂ gases as the H₂O source, and dimethyl zinc (DMZn) as the Zn source also will be carried out to grow the ZnO on graphene/insulator. One chemical approach acknowledged for its simple and low operation temperature, hydrothermal, is used to grow ZnO on the insulator in this study. The growth process will use low growth temperature at atmospheric pressure as the constant parameter.

1.5 Research Objective and Scopes

In this study, the main objective is to investigate the low-temperature growth of ZnO on an insulator by utilizing graphene as the buffer layer. The study will use physical and chemical techniques for the growth process of the insulator. In addition, the quality of ZnO structures will be thoroughly analyzed from their morphology, crystallinity and optical properties. There are three sub-objectives for achieving the goal.

- a) To synthesize and optimize the ZnO growth on an insulator utilizing a buffer layer using a combination of thermal evaporation PVD, hydrothermal, and a recent technique, hot water beam CVD.
- b) To compare the performances of the grown ZnO on graphene/insulator by its morphology, crystallinity, and optical properties.
- c) To analyze the best method for the ZnO on the insulator, utilizing a buffer layer.

This study concentrates on the growth of ZnO on an insulator using graphene as the buffer layer. The deposition and growth process will focus on low-temperature techniques using vapor and liquid phases; thermal evaporator PVD, hydrothermal, and hot water beam CVD. The effect of graphene on the grown ZnO has also been comprehensively studied. This study can be divided into four scopes, where three scopes are related to the growth techniques, and one scope for the second and third objective :

- i. The thermal evaporator PVD and oxidation process were combined in the deposition of ZnO on graphene on the insulator. ZnO's oxidation study was done with different oxidation times, 30 – 120 minutes, with a fixed temperature of 450°C. The as-deposited and oxidized deposited ZnO structures on buffered graphene were compared with non-buffered ZnO on the insulator. All finding was studied based on their morphology, crystallinity and optical properties.
- ii. The liquid phase technique, hydrothermal, was used in growing ZnO structures on the insulator. This study used three types of buffer layers for the grown ZnO: SLG, MLG, and ZnO seed layer. An equimolar solution of Zinc nitrate hexahydrate and HMTA was used to grow ZnO on all different buffer layers on the insulator. The grown ZnO was compared based on its morphology, crystallinity, and optical properties.
- iii. A relatively new method called hot water beam CVD was used to grow ZnO structures on graphene on an insulator. Here, SLG and MLG were used as the buffer layer. The high purity of O₂ and H₂ gases play a crucial part in forming hot water molecules with Pt catalyst. DMZn is used as the zinc source at fixed substrate temperature. A study on ZnO on an insulator utilizing a buffer layer by varying time and gas flow rates was evaluated. Effect on the quality of morphology, crystallinity, and optical properties of grown ZnO on different buffer layer graphene on insulators were analysed.
- iv. All the results are analyzed and compared by their performance on crystallinity and optical properties of the grown ZnO structures on the insulator, with and without a graphene buffer layer. The analyses were done to get the best technique to grow ZnO on an insulator utilizing graphene as the buffer.

1.6 Overview of Thesis Organization

This thesis consists of seven chapters and three chapters for results and discussions. Chapter 1 overviews the research background and its motivation for the growth of semiconductor material, ZnO, on insulator utilizing graphene as a template layer. The problem of the study has also been discussed in this section. Moreover, the research objective and its scope are also presented.

Chapter 2 gives an overview of the fundamental properties of ZnO and graphene. Discussion of previous studies of ZnO and buffer layer hybridisation on the insulator and their possible applications will be explained. In addition, growth techniques of ZnO structures on the insulator, especially in the thermal evaporator, hydrothermal, and catalyzed hot water beam and its previous study, are described in this chapter. The potential applications of oriented non-buffered ZnO nanostructures and ZnO nanostructures on graphene are also discussed.

Chapter 3 focuses on the research methodology. The substrate's properties and preparation prior to the experiment are presented. Three different methods used to grow ZnO structures are explained, and the parameters used during the study are also discussed. Preparation and techniques used to grow ZnO structures are presented. The characterization techniques used to study the grown ZnO are also listed.

Chapter 4 discussed the graphene factor to the grown ZnO on the insulator. A combination of thermal evaporator PVD and the oxidation process of the grown ZnO on graphene on an insulator will be discussed thoroughly. Besides, the comparison between grown ZnO on the insulator and grown ZnO on graphene on the insulator will be explained. The discussions will thoroughly examine the morphology, crystallinity and optical properties of the deposited ZnO on the insulator.

Chapter 5 studies the effect of buffer layers used to the grown ZnO on the insulator using the liquid-phase hydrothermal technique. Morphology, crystallinity and optical properties of the deposited ZnO on the insulator will be thoroughly discussed.

Chapter 6 introduces the new CVD method to grow high-quality ZnO. The method of the new CVD, hot water beam CVD, and the grown ZnO on graphene on the insulator will be explained. Morphology, crystallinity, and optical properties of grown ZnO on an insulator will be thoroughly discussed. Comparison between grown ZnO using thermal evaporator PVD, the hydrothermal technique and the new hot water beam CVD will also be explained here.

Finally, Chapter 7 concludes the contributions of the present works and discusses future research directions.

REFERENCES

1. Pillarisetty, R. Academic and industry research progress in germanium nanodevices. *Nature*, 2011. 479(7373): 324-328.
2. Zhang, G. Q. and Van Roosmalen. A. More than Moore: creating high value micro/nanoelectronics systems. *Springer Science & Business Media*, 2010.
3. Takagi, S., Sugiyama, M., Yasuda, T., and Takenaka, M. Ge/III-V channel engineering for future CMOS. *ECS Transactions*, 2009. 19(5): 9
4. Hashim, A. M., Anisuzzaman, M., Muta, S., Sadoh, T., and Miyao, M. Epitaxial-Template Structure Utilizing Ge-on-Insulator Stripe Arrays with Nanospacing for Advanced Heterogeneous Integration on Si Platform. *Japanese Journal of Applied Physics*, 2012. 51.
5. Ma, K., Urata, R., Miller, D. A., and Harria, J. S. Low-temperature growth of GaAs on Si used for ultrafast photoconductive switches. *IEEE journal of quantum electronics*, 2004. 40(6): 800-804.
6. Dadgar, A., Poschenrieder M., Bläsing J., Contreras, O., Bertram, F., Riemann, T., Reiher, A., Kunze, M., Daumiller, I., Krtschil, and A., Diez, A. MOVPE growth of GaN on Si (1 1 1) substrates. *Journal of Crystal Growth*, 2003. 248: 556-562.
7. Astuti, B., Tanikawa, M., Rahman, S. F. A., Yasui, K., and Hashim, A. M. Graphene as a Buffer Layer for Silicon Carbide-on-Insulator Structures. *Materials*, 2012. 5(11): 2270-2279.
8. Rusli, N. I., Tanikawa, M., Mahmood, M. R., Yasui, K., and Hashim, A. M. Growth of High-Density Zinc Oxide Nanorods on Porous Silicon by Thermal Evaporation. *Materials*, 2012. 5(12): 2817-2832.
9. Rahman, F. A., S., S. Kasai, and Hashim, A. M. Room temperature nonlinear operation of a graphene-based three-branch nanojunction device with chemical doping. *Applied Physics Letters*, 2012. 100(19).
10. Mazloumi, M., Mandal, H. S., and Tang, X. Fabrication of optical device arrays using patterned growth of ZnO nanostructures. *IEEE transactions on nanotechnology*, 2012. 11(3): 444-447.

11. Wang, J. and Lee, S. Ge-photodetectors for Si-based optoelectronic integration. *Sensors*, 2011. 11(1): 696-718.
12. Razykov, T. M., Ferekides, C. S., Morel, D., Stefanakos, E., Ullal, H. S., and Upadhyaya, H. M. Solar photovoltaic electricity: Current status and future prospects. *Solar energy*, 2011. 85(8): 1580-1608.
13. Ahn, M. W., Park, K. S., Heo, J. H., Park, J. G., Kim, D. W., Choi, K. J., Lee, J. H., and Hong, S. H. Gas sensing properties of defect-controlled ZnO-nanowire gas sensor. *Applied Physics Letters*, 2008. 93(26).
14. Young, D. J., Du, J., Zorman, C. A., and Ko, W. H. High-temperature single-crystal 3C-SiC capacitive pressure sensor. *IEEE sensors Journal*, 2004. 4(4): 464-470.
15. Burghartz, J. N. Thin chips on the ITRS roadmap, in Ultra-thin Chip Technology and Applications. *Springer*. 2011, 13-18.
16. Jo, J. W., Kang, S. H., Heo, J. S., Kim, Y. H., and Park, S. K. Flexible metal oxide semiconductor devices made by solution methods. *Chemistry—A European Journal*, 2020. 26(42): 9126-9156.
17. Jeong, J., Jin, D. K., Choi, J., Jang, J., Kang, B. K., Wang, Q., Park, W. I., Jeong, M. S., Bae, B. S., Yang, W.S., Kim, M. J., and Hong, Y. J. Transferable, flexible white light-emitting diodes of GaN p–n junction microcrystals fabricated by remote epitaxy. *Nano Energy*, 2021. 86: 106075.
18. Zhang, N., Sun, J., and Gong, H. Transparent p-type semiconductors: copper-based oxides and oxychalcogenides. *Coatings*, 2019. 9(2): 137.
19. Singh, P., Hu, L. L., Zan, H. W., and Tseng, T. Y. Highly sensitive nitric oxide gas sensor based on ZnO-nanorods vertical resistor operated at room temperature. *Nanotechnology*, 2019. 30(9): 095501.
20. Wu, J., Yin, C., Zhou, J., Li, H., Liu, Y., Shen, Y., Garner, S., Fu, Y., and Duan, H. Ultrathin glass-based flexible, transparent, and ultrasensitive surface acoustic wave humidity sensor with ZnO nanowires and graphene quantum dots. *ACS Applied Materials & Interfaces*, 2020. 12(35): 39817-39825.

21. Turemis, M., Zappi, D., Giardi, M. T., Basile, G., Ramanaviciene, A., Kapralovs, A., Ramanavicius, A., and Viter, R. ZnO/polyaniline composite based photoluminescence sensor for the determination of acetic acid vapor. *Talanta*, 2020. 211: 120658.
22. Jagadamma, L. K., Abdelsamie, M., El Labban, A., Aresu, E., Ndjawa, G. O. N., Anjum, D. H., Cha, D., Beaujuge, P. M., and Amassian, A. Efficient inverted bulk-heterojunction solar cells from low-temperature processing of amorphous ZnO buffer layers. *Journal of Materials Chemistry A*, 2014. 2(33): 13321-13331.
23. Koo, D., Jung, S., Seo, J., Jeong, G., Choi, Y., Lee, J., Lee, S. M., Cho, Y., Jeong, M., Lee, J. and Oh, J. Flexible Organic Solar Cells Over 15% Efficiency with Polyimide-Integrated Graphene Electrodes. *Joule*, 2020. 4(5): 1021-1034.
24. Royer, M., Holmen, J. O., Wurm, M. A., Aadland, O. S. and Glenn, M. ZnO on Si integrated acoustic sensor. *Sensors and Actuators*, 1983. 4: 357-362.
25. Sahare, P., Kumar, S., Kumar, S. and Singh, F. n-ZnO/p-Si heterojunction nanodiodes based sensor for monitoring UV radiation. *Sensors and Actuators A: Physical*, 2018. 279: 351-360.
26. Marsi, N., Majlis, B. Y., Hamzah, A. A. and Mohd-Yasin, F. Development of high temperature resistant of 500° C employing silicon carbide (3C-SiC) based MEMS pressure sensor. *Microsystem Technologies*, 2015. 21(2): 319-330.
27. Shur, M. GaN based transistors for high power applications. *Solid-State Electronics*, 1998. 42(12): 2131-2138.
28. Namavar, F. and Kalkhoran, N. M. High performance GaAs devices and method. *Google Patents*, 1995.
29. Baliga, B. J. Trends in power semiconductor devices. *IEEE Transactions on electron Devices*, 1996. 43(10): 1717-1731.

30. Pietruszka, R., Schifano, R., Krajewski, T. A., Witkowski, B. S., Kopalko, K., Wachnicki, L., Zielony, E., Gwozdz, K., Bieganski, P., Placzek-Popko, E. and Godlewski, M. Improved efficiency of n-ZnO/p-Si based photovoltaic cells by band offset engineering. *Solar Energy Materials and Solar Cells*, 2016. 147: 164-170.
31. Mukherjee, D., Reddy, B. V. R., Perveen, G., Kumar, N. and Noor, A. Comparison of three techniques for leakage current minimization in CMOS VLSI circuit in 90 nm technology. *International Journal of Recent Trends in Engineering and Technology*, 2020. 4(4):162-166.
32. Crabb, R. and Treble, F. Thin silicon solar cells for large flexible arrays. *Nature*, 1967. 213(5082): 1223-1224.
33. Park, J., Heo, S., Park, K., Song, M. H., Kim, J. Y., Kyung, G., Ruoff, R. S., Park, J. U. and Bien, F., Research on flexible display at Ulsan National Institute of Science and Technology. *npj Flexible Electronics*, 2017. 1(1): 1-13.
34. Shetti, N. P., Bukkitgar, S. D., Reddy, K. R., Reddy, C. V. and Aminabhavi, T. M. ZnO-based nanostructured electrodes for electrochemical sensors and biosensors in biomedical applications. *Biosens Bioelectron*, 2019. 141: 111417.
35. Bhattacharya, P., Fornari, R., and Kamimura, H. Comprehensive semiconductor science and technology. *Newnes*. 2011.
36. Hambali, N. A. and Hashim, A. M. Synthesis of Zinc Oxide Nanostructures on Graphene/Glass Substrate via Electrochemical Deposition: Effects of Potassium Chloride and Hexamethylenetetramine as Supporting Reagents. *Nanomicro Lett*, 2015. 7(4): 317-324.
37. Cai, S., Han, Z., Wang, F., Zheng, K., Cao, Y., Ma, Y. and Feng, X., Review on flexible photonics/electronics integrated devices and fabrication strategy. *Science China Information Sciences*, 2018. 61(6): 1-27.

38. Wang, X., Dong, L., Zhang, H., Yu, R., Pan, C. and Wang, Z. L., Recent progress in electronic skin. *Advanced Science*, 2015. 2(10): 1500169.
39. Novoselov, K., Mishchenko, O. A., Carvalho, O. A. and Castro Neto, A. H. 2D materials and van der Waals heterostructures. *Science*, 2016. 353(6298): aac9439.
40. Jeong, J., Jin, D. K., Cha, J., Kang, B. K., Wang, Q., Choi, J., Lee, S. W., Mikhailovskii, V. Y., Neplokh, V., Amador-Mendez, N. and Tchernycheva, M. Selective-area remote epitaxy of ZnO microrods using multilayer–monolayer-patterned graphene for transferable and flexible device fabrications. *ACS Applied Nano Materials*, 2020. 3(9): 8920-8930.
41. Thakar, K. and Lodha, S. Optoelectronic and photonic devices based on transition metal dichalcogenides. *Materials Research Express*, 2020. 7(1): 014002.
42. Prasada Rao, T., Santhosh Kumar, M. C., and Ganesan, V. Effect of annealing on the structural, optical and electrical properties of ZnO thin films by spray pyrolysis. *Indian Journal of Physics*, 2011. 85(9): 1381-1391.
43. Peguit, A. D. M. V., Candidato, R. T., Bagsican, F. R. G., Odarve, M. K. G., Jabian, M. E., Sambo, B. R. B., Vequizo, R. M. and Alguno, A. C. Growth of chemically deposited ZnO and ZnO-SiO₂ on Pt buffered Si substrate. in IOP Conference Series: Materials Science and Engineering. *IOP Publishing*. 2015.
44. Jayah, N. A., Yahaya, H., Mahmood, M. R., Terasako, T., Yasui, K. and Hashim, A. M. High electron mobility and low carrier concentration of hydrothermally grown ZnO thin films on seeded a-plane sapphire at low temperature. *Nanoscale research letters*, 2015. 10(1): 1-10.
45. Balandin, A. A., Ghosh, S., Bao, W., Calizo, I., Teweldebrhan, D., Miao, F. and Lau, C. N. Superior thermal conductivity of single-layer graphene. *Nano letters*, 2008. 8(3): 902-907.

46. Look, D. C., Recent advances in ZnO materials and devices. *Materials science and engineering: B*, 2001. 80(1-3): 383-387.
47. Singh, S. Zinc oxide nanostructures: Synthesis, characterizations and device applications. *Journal of Nanoengineering and Nanomanufacturing*, 2013. 3(4): 283-310.
48. Muhamad, A., Saito, T., Adachi, Y., Ono, S., Hashim, A. M. and Yasui, K. CVD growth of zinc oxide thin films on graphene on insulator using a high-temperature platinum-catalyzed water beam. *Journal of Materials Science*, 2018. 54(1): 228-237.
49. Ahmad, N. F., Rusli, N. I., Mahmood, M. R., Yasui, K. and Hashim, A. M., Seed/catalyst-free growth of zinc oxide nanostructures on multilayer graphene by thermal evaporation. *Nanoscale research letters*, 2014. 9(1): 1-7.
50. Abd Aziz, N. S., Nishiyama, T., Rusli, N. I., Mahmood, M. R., Yasui, K. and Hashim, A.M. Seedless growth of zinc oxide flower-shaped structures on multilayer graphene by electrochemical deposition. *Nanoscale research letters*, 2014. 9(1): 1-9.
51. Cook, B., Liu, Q., Liu, J., Gong, M., Ewing, D., Casper, M., Stramel, A. and Wu, J. Facile zinc oxide nanowire growth on graphene via a hydrothermal floating method: towards Debye length radius nanowires for ultraviolet photodetection. *J. Mater. Chem. C*, 2017. 5(38): 10087-10093.
52. Djurišić, A. B., Ng, A. M. C., and Chen, X. Y. ZnO nanostructures for optoelectronics: Material properties and device applications. *Progress in Quantum Electronics*, 2010. 34(4): 191-259.
53. Galdamez-Martinez, A., Santana, G., Güell, F., Martínez-Alanis, P. R. and Dutt, A., Photoluminescence of ZnO Nanowires: A Review. *Nanomaterials (Basel)*, 2020. 10(5): 857.

54. Yasui, K., Miura, H. and Nishiyama, H. Deposition of Zinc Oxide Thin Films Using a Surface Reaction on Platinum Nanoparticles. *MRS Proceedings*, 2011. 1315.
55. Agostini, G. and Lamberti, C. Characterization of semiconductor heterostructures and nanostructures. *Elsevier*, 2011.
56. Madou, M. J. Solid-State Physics, Fluidics, and Analytical Techniques in Micro-and Nanotechnology. *CRC Press*, 2011.
57. Özgür, Ü., Alivov, Y. I., Liu, C., Teke, A., Reshchikov, M., Doğan, S., Avrutin, V. C. S. J., Cho, S. J. and Morkoç, A. H. A comprehensive review of ZnO materials and devices. *Journal of applied physics*, 2005. 98(4): 11.
58. Huang, J., Z. Yin, and Zheng, Q. Applications of ZnO in organic and hybrid solar cells. *Energy & Environmental Science*, 2011. 4(10).
59. Zhang, P., Wu, J., Zhang, T., Wang, Y., Liu, D., Chen, H., Ji, L., Liu, C., Ahmad, W., Chen, Z. D. and Li, S. Perovskite Solar Cells with ZnO Electron-Transporting Materials. *Adv Mater*, 2018. 30(3).
60. Kaphle, A., Echeverria, E., McIlroy, D. N. and Hari, P., Enhancement in the performance of nanostructured CuO–ZnO solar cells by band alignment. *RSC Advances*, 2020. 10(13): 7839-7854.
61. Zhang, M., Zhang, H., Li, L., Tuokedaerhan, K. and Jia, Z. Er-enhanced humidity sensing performance in black ZnO-based sensor. *Journal of Alloys and Compounds*, 2018. 744: 364-369.
62. Shetti, N. P., Malode, S. J., Nayak, D. S., Bagihalli, G. B., Kalanur, S. S., Malladi, R. S., Reddy, C. V., Aminabhavi, T. M. and Reddy, K. R. Fabrication of ZnO nanoparticles modified sensor for electrochemical oxidation of methdilazine. *Applied Surface Science*, 2019. 496.
63. Cao, P., Yang, Z., Navale, S. T., Han, S., Liu, X., Liu, W., Lu, Y., Stadler, F. J. and Zhu, D. Ethanol sensing behavior of Pd-nanoparticles decorated

- ZnO-nanorod based chemiresistive gas sensors. *Sensors and Actuators B: Chemical*, 2019. 298.
64. Chen, Z., Yu, C., Shum, K., Wang, J. J., Pfenninger, W., Vockic, N., Midgley, J. and Kenney, J. T. Photoluminescence study of polycrystalline CsSnI₃ thin films: Determination of exciton binding energy. *Journal of Luminescence*, 2012. 132(2): 345-349.
 65. Saboor, A., Shah, S. M., and Hussain, H. Band gap tuning and applications of ZnO nanorods in hybrid solar cell: Ag-doped versus Nd-doped ZnO nanorods. *Materials Science in Semiconductor Processing*, 2019. 93: 215-225.
 66. Ridhuan, N. S., Abdul Razak, K., and Lockman, Z. Fabrication and Characterization of Glucose Biosensors by Using Hydrothermally Grown ZnO Nanorods. *Sci Rep*, 2018. 8(1): 13722.
 67. Fanny Chiat Orou, S., Hang, K. J., Thien, M. T., Ying, Y. L., Diem, N. D. N., Goh, B. H., Pung, S. Y. and Pung, Y. F. Antibacterial activity by ZnO nanorods and ZnO nanodisks: A model used to illustrate “Nanotoxicity Threshold”. *Journal of Industrial and Engineering Chemistry*, 2018. 62: 333-340.
 68. Li, C., Yu, L., Yuan, X., Li, Y., Ning, N., Cui, L., Ma, S., Kang, W. and Fan, X. Ag nanorods assembled with ZnO nanowalls for near-linear high-response UV photodetectors. *Journal of Alloys and Compounds*, 2020. 830.
 69. Kuo, K. Y., Chen, S. H., Hsiao, P. H., Lee, J. T. and Chen, C. Y. Day-night active photocatalysts obtained through effective incorporation of Au@Cu_xS nanoparticles onto ZnO nanowalls. *J Hazard Mater*, 2022. 421: 126674.
 70. Choi, K. S. and Chang, S. P. Effect of structure morphologies on hydrogen gas sensing by ZnO nanotubes. *Materials Letters*, 2018. 230: 48-52.

71. Park, S. J., Das, G. S., Schütt, F., Adelung, R., Mishra, Y. K., Tripathi, K. M. and Kim, T. Visible-light photocatalysis by carbon-nano-onion-functionalized ZnO tetrapods: degradation of 2,4-dinitrophenol and a plant-model-based ecological assessment. *NPG Asia Materials*, 2019. 11(1).
72. Kaviyarasu, K., Magdalane, C. M., Kanimozhi, K., Kennedy, J., Siddhardha, B., Reddy, E. S., Rotte, N. K., Sharma, C. S., Thema, F. T., Letsholathebe, D. and Mola, G.T. Elucidation of photocatalysis, photoluminescence and antibacterial studies of ZnO thin films by spin coating method. *J Photochem Photobiol B*, 2017. 173: 466-475.
73. Malik, G., Mourya, S., Jaiswal, J. and Chandra, R. Effect of annealing parameters on optoelectronic properties of highly ordered ZnO thin films. *Materials Science in Semiconductor Processing*, 2019. 100: 200-213.
74. Qin, L., Mawignon, F. J., Hussain, M., Ange, N. K., Lu, S., Hafezi, M. and Dong, G., Economic Friendly ZnO-Based UV Sensors Using Hydrothermal Growth: A Review. *Materials*, 2021. 14(15): 4083.
75. Coleman, V. A. and Jagadish, C. Basic properties and applications of ZnO, in Zinc oxide bulk, thin films and nanostructures. 2006, *Elsevier*. 1-20.
76. Fu, Y. Q., Luo, J. K., Du, X. Y., Flewitt, A. J., Li, Y., Markx, G. H., Walton, A. J. and Milne, W. I. Recent developments on ZnO films for acoustic wave based bio-sensing and microfluidic applications: a review. *Sensors and Actuators B: Chemical*, 2010. 143(2): 606-619.
77. Zagorac, D., Zagorac, J., Schoen, J. C., Stojanović, N. and Matović, B. ZnO/ZnS (hetero)structures: ab initio investigations of polytypic behavior of mixed ZnO and ZnS compounds. *Acta Crystallographica Section B Structural Science, Crystal Engineering and Materials*, 2018. 74(6): 628-642.
78. Ashrafi, A. A., Ueta, A., Avramescu, A., Kumano, H., Suemune, I., Ok, Y. W. and Seong, T. Y. Growth and characterization of hypothetical zinc-

- blende ZnO films on GaAs (001) substrates with ZnS buffer layers. *Applied Physics Letters*, 2000. 76(5): 550-552.
79. Munoz-Aguirre, N., Martínez-Pérez, L., Muñoz-Aguirre, S., Flores-Herrera, L. A., Vergara Hernández, E. and Zelaya-Angel, O. Luminescent Properties of (004) Highly Oriented Cubic Zinc Blende ZnO Thin Films. *Materials (Basel)*, 2019. 12(20).
 80. Rosales, A., Castaneda-Guzman, R., de Ita, A., Sánchez-Aké, C. and Pérez-Ruiz, S. J. Detection of zinc blende phase by the pulsed laser photoacoustic technique in ZnO thin films deposited via pulsed laser deposition. *Materials Science in Semiconductor Processing*, 2015. 34: 93-98.
 81. Rosales-Córdova, A., Castañeda-Guzmán, R., and Sanchez-Aké, C. Zinc blende phase detection in ZnO thin films grown with low doping Mn concentration by double-beam pulsed laser deposition. *Journal of Materials Science: Materials in Electronics*, 2018. 29(22): 18971-18977.
 82. Jaffe, J. E., Pandey, R., and Kunz, A. B. Electronic structure of the rocksalt-structure semiconductors ZnO and CdO. *Phys Rev B Condens Matter*, 1991. 43(17): 14030-14034.
 83. Saeed, Y., Shaukat, A., Ikram, N. and Tanveer, M. Structural and electronic properties of rock salt phase of ZnO under compression. *Journal of Physics and Chemistry of Solids*, 2008. 69(7): 1676-1683.
 84. Janotti, A. and Van de Walle, C. G. Fundamentals of zinc oxide as a semiconductor. *Reports on Progress in Physics*, 2009. 72(12).
 85. Amutha, A., Amirthapandian, S., Sundaravel, B., Panigrahi, B. K., Saravanan, K. and Thangadurai, P. Low-temperature photoluminescence behaviour of Ag decorated ZnO Nanorods. *Journal of Applied Physics*, 2016. 120(20).

86. Geim, A. K. and Novoselov, K. S. The rise of graphene, in Nanoscience and technology: a collection of reviews from nature journals. *World Scientific*. 2010, 11-19.
87. Novoselov, K. S., Geim, A. K., Morozov, S. V., Jiang, D., Katsnelson, M. I., Grigorieva, I., Dubonos, S. and Firsov, A. Two-dimensional gas of massless Dirac fermions in graphene. *Nature*, 2005. 438(7065): 197-200.
88. Wang, Y., Zhu, L., and Du, C. Flexible Difunctional (Pressure and Light) Sensors Based on ZnO Nanowires/Graphene Heterostructures. *Advanced Materials Interfaces*, 2020. 7(6).
89. Yadav, R. and Dixit, C. Synthesis, characterization and prospective applications of nitrogen-doped graphene: A short review. *Journal of Science: Advanced Materials and Devices*, 2017. 2(2): 141-149.
90. Wang, C., Wang, Z. G., Xi, R., Zhang, L., Zhang, S. H., Wang, L. J. and Pan, G. B. In situ synthesis of flower-like ZnO on GaN using electrodeposition and its application as ethanol gas sensor at room temperature. *Sensors and Actuators B: Chemical*, 2019. 292: 270-276.
91. Lee, Y. J., Yang, Z. P., Lo, F. Y., Siao, J. J., Xie, Z. H., Chuang, Y. L., Lin, T. Y. and Sheu, J. K. Slanted n-ZnO/p-GaN nanorod arrays light-emitting diodes grown by oblique-angle deposition. *APL Materials*, 2014. 2(5).
92. Tan, C., Cao, X., Wu, X. J., He, Q., Yang, J., Zhang, X., Chen, J., Zhao, W., Han, S., Nam, G. H. and Sindoro, M. Recent advances in ultrathin two-dimensional nanomaterials. *Chemical reviews*, 2017. 117(9): 6225-6331.
93. Park, H. J., Cha, J., Choi, M., Kim, J. H., Tay, R. Y., Teo, E. H. T., Park, N., Hong, S. and Lee, Z. One-dimensional hexagonal boron nitride conducting channel. *Science advances*, 2020. 6(10): eaay4958.
94. Chen, T. A., Chuu, C. P., Tseng, C. C., Wen, C. K., Wong, H. S. P., Pan, S., Li, R., Chao, T. A., Chueh, W. C., Zhang, Y. and Fu, Q. Wafer-scale

- single-crystal hexagonal boron nitride monolayers on Cu (111). *Nature*, 2020. 579(7798): 219-223.
95. Chung, K., Lee, C. H. and Yi, G. C. Transferable GaN layers grown on ZnO-coated graphene layers for optoelectronic devices. *Science*, 2010. 330(6004) :655-657.
 96. Hambali, N. A., Yahaya, H., Mahmood, M. R., Terasako, T. and Hashim, A. M. Synthesis of zinc oxide nanostructures on graphene/glass substrate by electrochemical deposition: effects of current density and temperature. *Nanoscale research letters*, 2014. 9(1): 1-7.
 97. Feng, Y., Zhang, Y., Song, X., Wei, Y. and Battaglia, V. S. Facile hydrothermal fabrication of ZnO–graphene hybrid anode materials with excellent lithium storage properties. *Sustainable Energy & Fuels*, 2017. 1(4): 767-779.
 98. Liang, F. X., Gao, Y., Xie, C., Tong, X. W., Li, Z. J. and Luo, L. B. Recent advances in the fabrication of graphene–ZnO heterojunctions for optoelectronic device applications. *Journal of Materials Chemistry C*, 2018. 6(15): 3815-3833.
 99. Chang, H., Sun, Z., Ho, K. Y. F., Tao, X., Yan, F., Kwok, W. M. and Zheng, Z. A highly sensitive ultraviolet sensor based on a facile in situ solution-grown ZnO nanorod/graphene heterostructure. *Nanoscale*, 2011. 3(1): 258-64.
 100. Yi, J., Lee, J. M., and Park, W. I. Vertically aligned ZnO nanorods and graphene hybrid architectures for high-sensitive flexible gas sensors. *Sensors and Actuators B: Chemical*, 2011. 155(1): 264-269.
 101. Boruah, B. D. Zinc oxide ultraviolet photodetectors: rapid progress from conventional to self-powered photodetectors. *Nanoscale Advances*, 2019. 1(6): 2059-2085.
 102. Liu, J. Y., Yu, X. X., Zhang, G. H., Wu, Y. K., Zhang, K., Pan, N. and Wang, X. P. High Performance Ultraviolet Photodetector Fabricated with

- ZnO Nanoparticles-graphene Hybrid Structures. *Chinese Journal of Chemical Physics*, 2013. 26(2): 225-230.
103. Liu, Q., Gong, M., Cook, B., Ewing, D., Casper, M., Stramel, A. and Wu, J. Transfer-free and printable graphene/ZnO-nanoparticle nanohybrid photodetectors with high performance. *Journal of Materials Chemistry C*, 2017. 5(26): 6427-6432.
 104. Li, X., Zhu, Y., Cai, W., Borysiak, M., Han, B., Chen, D., Piner, R.D., Colombo, L. and Ruoff, R. S. Transfer of large-area graphene films for high-performance transparent conductive electrodes. *Nano letters*, 2009. 9(12): 4359-4363.
 105. Yang, K., Xu, C., Huang, L., Zou, L. and Wang, H. Hybrid nanostructure heterojunction solar cells fabricated using vertically aligned ZnO nanotubes grown on reduced graphene oxide. *Nanotechnology*, 2011. 22(40): 405401.
 106. Zhang, Y., Ram, M. K., Stefanakos, E. K. and Goswami, D. Y. Synthesis, characterization, and applications of ZnO nanowires. *Journal of Nanomaterials*, 2012. 2012.
 107. Srujana, S. and Bhagat, D. Chemical-based synthesis of ZnO nanoparticles and their applications in agriculture. *Nanotechnology for Environmental Engineering*, 2022. 7(1): 269-275
 108. Wang, F., Zhao, H., Liang, J., Li, T., Luo, Y., Lu, S., Shi, X., Zheng, B., Du, J. and Sun, X. Magnetron sputtering enabled synthesis of nanostructured materials for electrochemical energy storage. *Journal of Materials Chemistry A*, 2020. 8(39): 20260-20285.
 109. Saha, J. K., Bukke, R. N., Mude, N. N. and Jang, J. Significant improvement of spray pyrolyzed ZnO thin film by precursor optimization for high mobility thin film transistors. *Scientific reports*, 2020. 10(1): 1-11.

110. Wang, H., Maiyalagan, T., and Wang, X. Review on recent progress in nitrogen-doped graphene: synthesis, characterization, and its potential applications. *AcS catalysis*, 2012. 2(5): 781-794.
111. Ghafouri, V., Ebrahimzad, A., and Shariati, M. The effect of annealing time and temperature on morphology and optical properties of ZnO nanostructures grown by a self-assembly method. *Scientia Iranica*, 2013. 20(3): 1039-1048.
112. Kim, K. H., Utashiro, K., Abe, Y. and Kawamura, M. Growth of zinc oxide nanorods using various seed layer annealing temperatures and substrate materials. *Int. J. Electrochem. Sci.*, 2014. 9(2014): 2080-2089.
113. Liu, J., Lv, Y., Zhang, W., Zhang, Z. and Wang, A. Tailoring the structural and optical properties of RF magnetron sputtered ZnO/graphene thin films by annealing temperature. *Integrated Ferroelectrics*, 2019. 198(1): 142-152.
114. Byrappa, K. and Adschiri, T. Hydrothermal technology for nanotechnology. *Progress in crystal growth and characterization of materials*, 2007. 53(2): 117-166.
115. Barka-Bouaifel, F., Sieber, B., Bezzi, N., Benner, J., Roussel, P., Boussekey, L., Szunerits, S. and Boukherroub, R. Synthesis and photocatalytic activity of iodine-doped ZnO nanoflowers. *Journal of Materials Chemistry*, 2011. 21(29): 10982-10989.
116. Wahid, K. A., Lee, W. Y., Lee, H. W., Teh, A. S., Bien, D. C. and Abd Azid, I. Effect of seed annealing temperature and growth duration on hydrothermal ZnO nanorod structures and their electrical characteristics. *Applied Surface Science*, 2013. 283: 629-635.
117. Tao, Y., Fu, M., Zhao, A., He, D. and Wang, Y. The effect of seed layer on morphology of ZnO nanorod arrays grown by hydrothermal method. *Journal of Alloys and compounds*, 2010. 489(1): 99-102.

118. Qin, F. F., Xu, C. X., Zhu, Q. X., Lu, J. F., Chen, F., You, D. T., Zhu, Z. and Manohari, A. G. Optical performance improvement in hydrothermal ZnO/graphene structures for ultraviolet lasing. *Journal of Materials Chemistry C*, 2018. 6(13): 3240-3244.
119. Meng, F., Chang, Y., Qin, W., Yuan, Z., Zhao, J., Zhang, J., Han, E., Wang, S., Yang, M., Shen, Y. and Ibrahim, M. ZnO-Reduced Graphene Oxide Composites Sensitized with Graphitic Carbon Nitride Nanosheets for Ethanol Sensing. *ACS Applied Nano Materials*, 2019. 2(5): 2734-2742.
120. Hang, T., Wu, J., Xiao, S., Li, B., Li, H., Yang, C., Yang, C., Hu, N., Xu, Y., Zhang, Y. and Xie, X. Anti-biofouling NH₃ gas sensor based on reentrant thorny ZnO/graphene hybrid nanowalls. *Microsystems & nanoengineering*, 2020. 6(1): 1-11.
121. Nishiyama, H., Miura, H., Yasui, K. and Inoue, Y. Fabrication of high-electron-mobility ZnO epilayers by chemical vapor deposition using catalytically produced excited water. *Journal of Crystal Growth*, 2010. 312(4): 483-486.
122. Yasui, K., Nishiyama, H., Tsukichi, M., Inoue, Y. and Takata, M. Fabrication method and fabrication apparatus for fabricating metal oxide thin film. *Google Patents*, 2013.
123. Saito, T., Kato, A. and Yasui, K. Defect distribution in ZnO thin films grown on a-plane sapphire substrates by catalytic-reaction-assisted chemical vapor deposition. *Journal of Crystal Growth*, 2021. 570: 126206.
124. Nagatomi, E., Satomoto, S., Tahara, M., Kato, T. and Yasui, K. Optical properties of ZnO thin films grown on glass substrates using catalytically generated high-temperature H₂O. *Surface and Coatings Technology*, 2013. 215: 148-151.
125. Kato, A., Satomoto, S., Tahara, M., Kato, T. and Yasui, K. Polarization properties of nonpolar ZnO films grown on R-sapphire substrates using high-temperature H₂O generated by a catalytic reaction. *Thin Solid Films*, 2017. 644: 29-32.

126. Ferrari, A. C., Meyer, J. C., Scardaci, V., Casiraghi, C., Lazzeri, M., Mauri, F., Piscanec, S., Jiang, D., Novoselov, K. S., Roth, S. and Geim, A. K. Raman spectrum of graphene and graphene layers. *Phys Rev Lett*, 2006. 97(18): 187401.
127. Ferrari, A. C. and Basko, D. M. Raman spectroscopy as a versatile tool for studying the properties of graphene. *Nat Nanotechnol*, 2013. 8(4): 235-46.
128. Kaniyoor, A. and Ramaprabhu, S. A Raman spectroscopic investigation of graphite oxide derived graphene. *AIP Advances*, 2012. 2(3).
129. Salifairus, M. J., Abd Hamid, S. B., Soga, T., Alrokayan, S. A., Khan, H. A. and Rusop, M. Structural and optical properties of graphene from green carbon source via thermal chemical vapor deposition. *Journal of Materials Research*, 2016. 31(13): 1947-1956.
130. Zhang, J., Cui, X., Shi, Z., Wu, B., Zhang, Y. and Zhang, B. Nucleation and growth of ZnO films on Si substrates by LP-MOCVD. *Superlattices and Microstructures*, 2014. 71: 23-29.
131. Srivatsa, K., Chhikara, D. and Kumar, M. S. Synthesis of aligned ZnO nanorod array on silicon and sapphire substrates by thermal evaporation technique. *Journal of Materials Science & Technology*, 2011. 27(8): 701-706.
132. Xu, S. and Wang, Z. L. One-dimensional ZnO nanostructures: solution growth and functional properties. *Nano Research*, 2011. 4(11): 1013-1098.
133. Amin, G., Asif, M. H., Zainelabdin, A., Zaman, S., Nur, O. and Willander, M. Influence of pH, precursor concentration, growth time, and temperature on the morphology of ZnO nanostructures grown by the hydrothermal method. *Journal of Nanomaterials*, 2011.
134. Zainelabdin, A., Zaman, S., Amin, G., Nur, O. and Willander, M. Deposition of well-aligned ZnO nanorods at 50 C on metal, semiconducting polymer, and copper oxides substrates and their structural and optical properties. *Crystal Growth & Design*, 2010. 10(7): 3250-3256.

135. Ladanov, M., Ram, MK., Matthews, G. and Kumar, A. Structure and opto-electrochemical properties of ZnO nanowires grown on n-Si substrate. *Langmuir*, 2011. 27(14): 9012-9017.
136. Abdullah, N., Ismail, N. M. and Nuruzzaman, D. M. The Influence of Growth Temperature on The Properties of Zinc Oxide by Thermal Oxidation. *Malaysian Journal of Analytical Sciences*, 2018. 22(6): 1084-1089.
137. Hojabri, A., Hajakbari, F. and Ghodrat, Y. Thermal Oxidation Times Effect on Structural and Morphological Properties of Molybdenum Oxide Thin Films Grown on Quartz Substrates. *Journal of Applied Chemical Research*, 2015. 9(4): 103-111.
138. Yu, W. and Pan, C. Low temperature thermal oxidation synthesis of ZnO nanoneedles and the growth mechanism. *Materials Chemistry and Physics*, 2009. 115(1): 74-79.
139. Yuan, L., Wang, C., Cai, R., Wang, Y. and Zhou, G. Temperature-dependent growth mechanism and microstructure of ZnO nanostructures grown from the thermal oxidation of zinc. *Journal of Crystal Growth*, 2014. 390: 101-108.
140. Yang, L. L. Synthesis and Characterization of ZnO nanostructures. *Linköping University Electronic Press*, 2010
141. Ledoux, G., Guillois, O., Huisken, F., Kohn, B., Porterat, D. and Reynaud, C. Crystalline silicon nanoparticles as carriers for the Extended Red Emission. *Astronomy & Astrophysics*, 2001. 377(2): 707-720.
142. Amirzada, M.R., Tatzel, A., Viereck, V. and Hillmer, H. Surface roughness analysis of SiO₂ for PECVD, PVD and IBD on different substrates. *Applied Nanoscience*, 2016. 6(2); 215-222.
143. Kim, H. W. and Kim, N. H. Annealing effect for structural morphology of ZnO film on SiO₂ substrates. *Materials Science in Semiconductor Processing*, 2004. 7(1-2): 1-6.

144. Humphreys, F. J. and Hatherly, M. Recrystallization and related annealing phenomena. *Elsevier*, 2012.
145. Bruncko, J., Vincze, A., Netrvalova, M., Šutta, P., Hasko, D. and Michalka, M. Annealing and recrystallization of amorphous ZnO thin films deposited under cryogenic conditions by pulsed laser deposition. *Thin solid films*, 2011. 520(2): 866-870.
146. Vyas, S., Giri, P., Singh, S. and Chakrabarti, P. Comparative study of as-deposited ZnO thin films by thermal evaporation, pulsed laser deposition and RF sputtering methods for electronic and optoelectronic applications. *Journal of Electronic Materials*, 2015. 44(10): 3401-3407.
147. Faraj, M. and Ibrahim, K. Optical and structural properties of thermally evaporated zinc oxide thin films on polyethylene terephthalate substrates. *International Journal of Polymer Science*, 2011.
148. Son, H., Choi, Y. J., Hwang, J. and Jeon, D. W. Influence of post-annealing on properties of α -Ga₂O₃ epilayer grown by halide vapor phase epitaxy. *ECS Journal of Solid State Science and Technology*, 2019. 8(7): Q3024.
149. Morshed, T., Kai, Y., Matsumura, R., Park, J. H., Chikita, H., Sadoh, T. and Hashim, A.M. Formation of large-grain crystalline germanium on single layer graphene on insulator by rapid melting growth. *Materials Letters*, 2016. 178: 147-150.
150. Do, T. A. T., Giang, H. T., Ngan, P. Q., Thai, G. H. and Dai Lam, T. Correlation between photoluminescence spectra with gas sensing and photocatalytic activities in hierarchical ZnO nanostructures. *RSC advances*, 2017. 7(16): 9826-9832.
151. Song, J. and Lim, S. Effect of seed layer on the growth of ZnO nanorods. *The Journal of Physical Chemistry C*, 2007. 111(2): 596-600.
152. Zhang, N., Zhang, Y. and Xu, Y. J. Recent progress on graphene-based photocatalysts: current status and future perspectives. *Nanoscale*, 2012. 4(19): 5792-5813.

153. Yang, M. Q., Zhang, N., Pagliaro, M. and Xu, Y. J. Artificial photosynthesis over graphene–semiconductor composites. Are we getting better? *Chemical Society Reviews*, 2014. 43(24): 8240-8254.
154. Aziz, N. S. A., Mahmood, M. R., Yasui, K. and Hashim, A. M., Seed/catalyst-free vertical growth of high-density electrodeposited zinc oxide nanostructures on a single-layer graphene. *Nanoscale research letters*, 2014. 9(1), 1-7.
155. Kim, Y. J., Yoon, A., Kim, M., Yi, G. C. and Liu, C. Hydrothermally grown ZnO nanostructures on few-layer graphene sheets. *Nanotechnology*, 2011. 22(24): 245603.
156. Hong, H. K., Jo, J., Hwang, D., Lee, J., Kim, N. Y., Son, S., Kim, J. H., Jin, M. J., Jun, Y. C., Erni, R. and Kwak, S. K. Atomic scale study on growth and heteroepitaxy of ZnO monolayer on graphene. *Nano letters*, 2017. 17(1): 120-127.
157. Rajamanickam, S., Mohammad, S. M. and Hassan, Z. Effect of zinc acetate dihydrate concentration on morphology of ZnO seed layer and ZnO nanorods grown by hydrothermal method. *Colloid and Interface Science Communications*, 2020. 38: 100312.
158. Wibowo, A., Marsudi, M. A., Amal, M. I., Ananda, M. B., Stephanie, R., Ardy, H. and Diguna, L. J. ZnO nanostructured materials for emerging solar cell applications. *RSC advances*, 2020. 10(70): 42838-42859.
159. Amutha, A., Amirthapandian, S., Sundaravel, B., Panigrahi, B. K., Saravanan, K. and Thangadurai, P. Low-temperature photoluminescence behaviour of Ag decorated ZnO Nanorods. *Journal of Applied Physics*, 2016. 120(20): 205104.
160. Kim, M. S., Yim, K. G., Leem, J. Y., Kim, S., Nam, G., Lee, D. Y., Kim, J. S. and Kim, J. S. Thickness Dependence of Properties of ZnO Thin Films on Porous Silicon Grown by Plasma-assisted Molecular Beam Epitaxy. *Journal of the Korean Physical Society*, 2011. 59(3): 2354-2361.

161. Fragalà, M. E., Di Mauro, A., Cristaldi, D. A., Cantarella, M., Impellizzeri, G. and Privitera, V. ZnO nanorods grown on ultrathin ZnO seed layers: Application in water treatment. *Journal of Photochemistry and Photobiology A: Chemistry*, 2017. 332: 497-504.
162. Nur Azzyaty binti Jayah. Seeded Growth of Zinc Oxide Thin Film and Nanostructure by Hydrothermal Method. Master thesis. Universiti Teknologi Malaysia. 2011
163. Liu, L., Ryu, S., Tomasik, M. R., Stolyarova, E., Jung, N., Hybertsen, M. S., Steigerwald, M. L., Brus, L. E. and Flynn, G. W. Graphene oxidation: thickness-dependent etching and strong chemical doping. *Nano letters*, 2008. 8(7): 1965-1970.
164. Ahmad, N. F., Yasui, K. and Hashim, A. M. Seed/catalyst-free growth of zinc oxide on graphene by thermal evaporation: effects of substrate inclination angles and graphene thicknesses. *Nanoscale Res Lett*, 2015. 10: 10.
165. Schubert, M. Infrared ellipsometry on semiconductor layer structures: phonons, plasmons, and polaritons. *Springer Science & Business Media*, 2004. 209.
166. Kanauchi, S., Ohashi, Y., Ohishi, K., Katagiri, H., Tamayama, Y., Kato, T. and Yasui, K. Effect of N₂O-doped buffer layer on the optical properties of ZnO films grown on glass substrates using high-energy H₂O generated by catalytic reaction. *Japanese Journal of Applied Physics*, 2016. 55(2S).
167. Ibach, H. Thermal expansion of silicon and zinc oxide (II). *Physica status solidi (b)*, 1969. 33(1): 257-265.
168. Yoon, D., Son, Y. W. and Cheong, H. Negative thermal expansion coefficient of graphene measured by Raman spectroscopy. *Nano Lett*, 2011. 11(8): 3227-31.

169. Hamid Ghasemi, A .R. Thermal expansion coefficient of graphene using molecular dynamics simulation: A comparative study on potential functions. *Journal of Physics: Conference Series*, 2017. 785: 7.
170. Morshed, T., Kai, Y., Matsumura, R., Park, J. H., Chikita, H., Sadoh, T. and Hashim, A. M. Formation of germanium (111) on graphene on insulator by rapid melting growth for novel germanium-on-insulator structure. *Materials Letters*, 2016. 168: 223-227.

LIST OF PUBLICATIONS

1. **Muhamad A**, Saito T, Adachi Y, Ono S, Hashim A. M, and Yasui K. CVD growth of zinc oxide thin films on graphene on insulator using a high-temperature platinum-catalyzed water beam. *Journal of Materials Science*. 2019. 54(1):228-37.